Applied and Environmental Microbiology, Apr. 2011, p. 2640–2647 Vol. 77, No. 8
0099-2240/11/$12.00 doi:10.1128/AEM.01460-10

Kinetics of Hydrothermal Inactivation of Endotoxins[▽]

Lixiong Li,* Chris L. Wilbur, and Kathryn L. Mintz

Applied Research Associates, Inc., 430 West 5th Street, Suite 700, Panama City, Florida 32401

Received 18 June 2010/Accepted 17 December 2010

A kinetic model was established for the inactivation of endotoxins in water at temperatures ranging from 210°C to 270°C and a pressure of 6.2×10^6 Pa. Data were generated using a bench scale continuous-flow reactor system to process feed water spiked with endotoxin standard (*Escherichia coli* O113:H10). Product water samples were collected and quantified by the *Limulus* amebocyte lysate assay. At 250°C, 5-log endotoxin inactivation was achieved in about 1 s of exposure, followed by a lower inactivation rate. This non-log-linear pattern is similar to reported trends in microbial survival curves. Predictions and parameters of several non-log-linear models are presented. In the fast-reaction zone (3- to 5-log reduction), the Arrhenius rate constant fits well at temperatures ranging from 120°C to 250°C on the basis of data from this work and the literature. Both biphasic and modified Weibull models are comparable to account for both the high and low rates of inactivation in terms of prediction accuracy and the number of parameters used. A unified representation of thermal resistance curves for a 3-log reduction and a 3 *D* value associated with endotoxin inactivation and microbial survival, respectively, is presented.

The connection between pyrogens and fevers in patients who receive unsanitized intravenous fluids was first reported by Florence Seibert in the 1920s (32). One subset of pyrogens is bacterial endotoxins which cause the pyrogenic reactions. Endotoxins come from the outer membrane of the cell wall of Gram-negative bacteria. Endotoxins are polymeric materials represented by lipopolysaccharides (LPS) having a number average molecular weight on the order of 10,000. The active sites in endotoxins are known as lipid A (29).

Pyrogen-free water is an essential material for the medical and pharmaceutical industries. Commonly known as water for injection (WFI) and sterile WFI (SWFI), the specifications require the removal of dissolved and suspended solids, sterilization, and depyrogenation (38). Distillation is the oldest method of producing pyrogen-free water (33). Distillation requires heat to separate pure water from its high boiling point impurities: inorganic solids, microorganisms, pyrogens, and all organics with boiling points higher than the operating temperature. The process also achieves sterilization of the product water. Because of energy intensity, heat recuperation by vapor compression or multiple-effect distillation is required to make the process economical.

Reverse osmosis (RO) is used industrially to produce WFI in Japan (22). The RO process relies on semipermeable membranes to remove impurities from water. Due to the possibilities of membrane defects, two-stage RO is required. Since there is no heat involved in the RO process, the product water is considered WFI, unless the water is posttreated by proven methods to ensure its sterility.

The thermal sterilization and depyrogenation techniques can be achieved by either wet heat or dry heat. In a wet heat application such as the commonly practiced autoclave steam sterilization technique, 3 orders of magnitude of microbial reduction (known as the 3 *D* value) is typically achieved at 121°C for 18 min or 134°C for 3 min (21). For dry heat to achieve the 3 *D* value, it requires 3 h at 140°C or 1 h at 170°C (15, 34). Dry heat depyrogenation for a 3-log reduction of endotoxin requires 250°C for 30 min (41). Dry heat is considered an oxidative process—almost like a combustion process (13). If effective dry heat depyrogenation is performed, sterilization generally is achieved as well. Depyrogenation can also be achieved by moist heat (4, 5, 20, 28) and in condensed high-temperature water (25). The former typically involves temperatures of 121°C to 150°C under saturated conditions, and the latter has extended the temperature from 150°C to 400°C under pressures that prevent water from boiling. Since the properties of water under high-temperature and high-pressure conditions undergo changes from polar to nonpolar characteristics, the impact of high-temperature water on the inactivation of endotoxin is evaluated.

The purposes of this study were 3-fold, (i) to generate endotoxin inactivation rate data upon which a kinetic model can be based for scaling up high-temperature hydrothermal processing (HTP) to produce SWFI, (ii) to interpret the data generated in this study by analyzing mechanisms of endotoxin inactivation by dry heat and moist heat, and (iii) to establish a unified representation of the thermal resistance curves for depyrogenation and sterilization by dry heat, moist heat, and HTP processes.

MATERIALS AND METHODS

Materials and supplies. The primary feed water (or supply water) used was generated on site using a standard RO and deionization system. The endotoxin feed water used was created by using commercially available SWFI, USP (NDC 0110302647850107; B. Braun), spiked with USP endotoxin standard *Escherichia coli* O113:H10 (Associates of Cape Cod, Inc. [ACCI], East Falmouth, MA). Control standard endotoxin (CSE) was reconstituted with 10 ml of commercial SWFI (B. Braun). The endotoxin feed was added to the supply water at a ratio of 1:50. CSE can be obtained in microgram or nanogram quantities per vial. The conversion of nanogram quantities to endotoxin units (EU) per ml accounts for both the potency and volume of the solution used for reconstitution. The potency

* Corresponding author. Mailing address: Applied Research Associates, Inc., 430 West 5th Street, Suite 700, Panama City, FL 32401. Phone: (850) 914-3188. Fax: (850) 914-3189. E-mail: lli@ara.com.

▽ Published ahead of print on 30 December 2010.

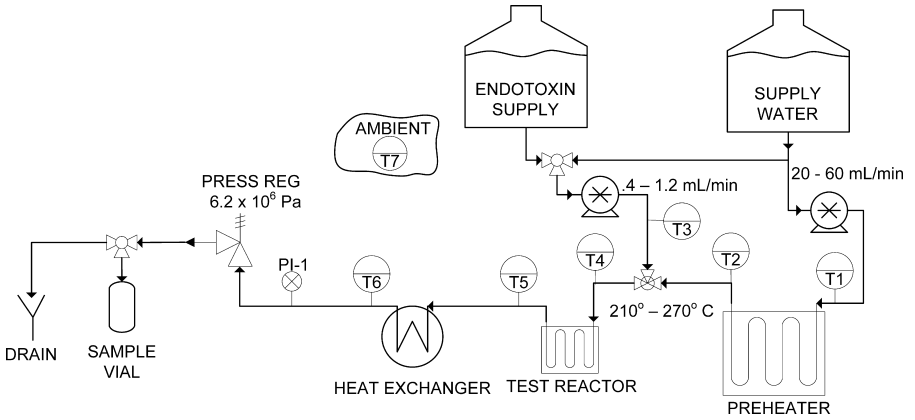

FIG. 1. Schematic of the bench scale continuous-flow HTP system used in this study.

of a CSE is defined as a measure of its activity relative to the activity of the reference standard endotoxin (RSE) in EU per ml. Commonly, the potency of a CSE is expressed as EU of RSE per ng of CSE and varies from 2 to 50 EU/ng. Sterile, endotoxin-free sample collection vials (model STERCL10) were obtained from Research Laboratory Supply, Inc.

Cleaning procedure. The system was cleaned by running source water for extended periods of time. Samples SDD-03-16, SDD-03-23, and SDD-03-31 represent source water flowing through a hot, "clean" system.

LAL assay. Quantitative detection of bacterial endotoxins is accomplished by the widely accepted *Limulus* amebocyte lysate (LAL) assay (37). Determination of the endotoxin concentrations of standards and samples was performed at ACCI using either the gel clot or endpoint turbidimetric technique of the USP <85> bacterial endotoxin test. Because the concentration of endotoxin standards was relatively low, a special effort was made to identify and minimize possible interference during every step of the experiments. Interference with the LAL assay is classified into two categories: inhibition and enhancement (16). In this study, inhibition was a greater concern because such data would falsely imply the safety of hydrothermal systems. There are two possible sources of interference that could affect or reduce the LAL readings as the primary indication of endotoxin reduction in this study. The first interference is the absorption or retention of endotoxin standards that could take place within the test systems. Results from the preliminary experiments described below demonstrated that the loss of endotoxin standards due to adsorption or retention was identified, controlled, and verified to be acceptable within the range of experimental error. Alternatively, the second interference could be an artifact resulting from a change in the lipid A structure due to heat, pressure, and water affecting the sensitivity of the LAL test to the remaining endotoxin. No literature was found to show evidence that the change in structure would result in a lower LAL reading.

Apparatus and operating procedure. A flow diagram of the bench scale HTP system is shown in Fig. 1. The key components of the test reactor system include pumps (Lab Alliance Prep 100 pump P40SFT01 and Waters model 510), a preheater, a reactor, a heat exchanger, and a pressure regulator. The preheater was used to heat the supply water to the desired operating temperature to ensure an isothermal temperature profile in the reactor. Both the preheater and the reactor were submersed in a variable-temperature fluidized sand bath. The preheater was fabricated from 3 m of 316 stainless steel tubing with an outside diameter of 3.18 mm and an inside diameter of 1.75 mm. The reactor was fabricated from 316 stainless steel tubing with an outside diameter of 1.60 mm and an inside diameter of 0.58 mm. The pressure regulator was used to keep the system pressure greater than the saturation pressure. A pressure gauge (range, 0 to 70 $\times$ 10^5 Pa; Wika) was used to monitor system pressure. Thermocouples (Omega EQSS-116U-12) were used throughout the system to monitor system temperature.

The supply water and the endotoxin feed solution were pumped through the system simultaneously. The supply water source was fed through the system at 20 to 60 ml/min. The endotoxin solution was fed through the system at 0.4 to 1.2 ml/min. A volumetric flow ratio of 1:50 was selected to minimize the impact of a temperature change due to cold endotoxin solution injection into the preheated water stream. The endotoxin solution was injected into the primary stream after the supply water had been preheated. The combined solution passed through the test reactor, which maintained the fluid at the desired operating temperature. Exiting the test reactor, the fluid was cooled and collected via the sample vial or discarded as waste.

Reactor/heat exchanger design and residence time. To minimize the amount of endotoxin required to perform these tests, the test reactor was designed to operate at relatively low flow rates as indicated above. Since the primary goal of this study was to generate kinetic data for scaling up of the hydrothermal process system, the impact of the heat transfer, fluid-mixing, and turbulent-flow characteristics due to reactor size and flow rate had to be considered. Based on similarity rules governing reactor scale-up, the test reactor was operated at the feed water flow rate that corresponds to a Reynolds number of 7,000 to 21,000. Since the transition from laminar-flow to turbulent-flow regions occurs between Reynolds numbers of 2,000 and 4,000, a region called the critical zone (3), the turbulent-flow regimen was achieved under these conditions. For example, at 250°C and 25 ml/min, the Reynolds number of water flowing through the test reactor is 8,550, which is well beyond the critical zone and comparable to what is required for a targeted scale-up system with a Reynolds number of 10,200 at 14 liters/h and 250°C.

The heat exchanger was of a tube-in-tube design and was used to quench the reactor effluent. It was 1,143 mm long and constructed of a 6.35-mm-diameter shell tube and a 1.59-mm-diameter inner tube. The outlet temperature of the heat exchanger was monitored via T6 (thermocouple 6) as illustrated in Fig. 1. This temperature did not exceed 28°C. Figure 2 illustrates the calculated temperatures as a function of time within the heat exchanger. Within approximately 0.1 s, the temperature of the spiked water is quenched to less than 175°C for 20 ml/min. At higher feed water flow rates, the temperature drop is more rapid, suggesting that the reaction is effectively quenched.

The endotoxin inactivation kinetics study focused on establishing the correlation between the reactor residence time at a given temperature with a measured endotoxin concentration in the effluent water sample. Table 1 is the test matrix

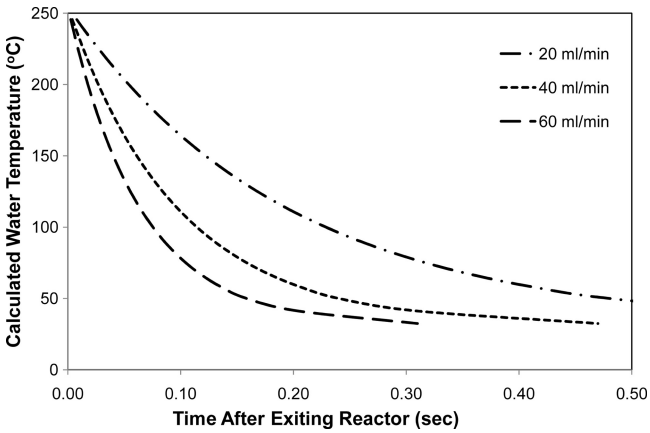

FIG. 2. Predicted temperature profile of water passing through a heat exchanger.

TABLE 1. Reactor dimensions, test conditions, and results

Reactor length (m) and sample	Temp (°C)	Flow rate (ml/min)		Residence time (s)	Endotoxin concn (EU/ml)	Endotoxin remaining (%)	Note
		Total	Endotoxin				
0.61							
SDD-03-01	270	30.0	0.0	0.33	0.0713		Water
SDD-03-02	270	30.3	0.3	0.32	0.288	5.1	Endotoxin
SDD-03-03	270	40.4	0.4	0.24	0.474	8.4	Endotoxin
SDD-03-04	240	30.3	0.3	0.32	0.468	8.3	Endotoxin
SDD-03-05	240	20.2	0.2	0.49	1.58	28.1	Endotoxin
SDD-03-06	Ambient	30.0	0.0	0.33	6.94		Water
SDD-03-07	Ambient	20.2	0.2	0.49	5.63	100.0	Endotoxin
NA							
SDD-03-08	Ambient	NA[a]	NA	NA	549,750	NA	Source vial
0.61							
SDD-03-09	Ambient	30.0	0.0	NA	0.25	NA	Water
SDD-03-10	Ambient	30.0	0.6	NA	1,300	NA	Endotoxin
SDD-03-11	Ambient	30.0	0.6	NA	2,500	NA	Endotoxin
SDD-03-12	Ambient	30.0	0.6	NA	2,500	NA	Endotoxin
SDD-03-13	Ambient	30.0	0.6	NA	2,500	NA	Endotoxin, TEA
SDD-03-14	Ambient	30.0	0.0	NA	100 & 100[b]	NA	TEA
NA							
SDD-03-15	Ambient	0.0	0.0	NA	3,500	NA	Feed source
1.22							
SDD-03-16	250	20.0	0.0	0.94	0.023	0.001	Water
SDD-03-17	250	20.0	0.4	0.94	0.276	0.007	Endotoxin
SDD-03-18	250	20.0	0.4	0.94	0.852	0.021	Endotoxin
SDD-03-19	250	40.0	0.8	0.47	32.9	0.823	Endotoxin
SDD-03-20	250	60.0	1.2	0.31	129	3.225	Endotoxin
SDD-03-21	250	60.0	1.2	0.31	131	3.275	Endotoxin
SDD-03-22	Ambient	40.0	0.8	NA	1,560	*[c]	Feed source
3.66							
SDD-03-23	270	30.0	0.0	1.88	<0.010	0.0002	Water
SDD-03-24	270	30.0	0.6	1.88	0.0170	0.0004	Endotoxin
SDD-03-25	270	40.0	0.8	1.41	0.1060	0.0026	Endotoxin
SDD-03-26	270	50.0	1.0	1.13	0.0480	0.0012	Endotoxin
SDD-03-27	250	20.0	0.4	2.81	0.008	0.0002	Endotoxin
SDD-03-28	250	30.0	0.6	1.88	0.012	0.0003	Endotoxin
SDD-03-29	250	40.0	0.8	1.41	0.033	0.0008	Endotoxin
SDD-03-30	Ambient	20.0	0.4	NA	4,020	100	Feed source
SDD-03-31	230	20.0	0.0	2.81	0.070	0.0016	Water
SDD-03-32	230	20.0	0.4	2.81	6.14	0.14	Endotoxin
SDD-03-33	230	35.0	0.7	1.61	22.6	0.52	Endotoxin
SDD-03-34	230	50.0	1.0	1.13	46.6	1.07	Endotoxin
SDD-03-35	210	20.0	0.4	2.81	149	3.4	Endotoxin
SDD-03-36	210	35.0	0.7	1.61	864	19.9	Endotoxin
SDD-03-37	210	50.0	1.0	1.13	699	16.1	Endotoxin
SDD-03-38	Ambient	20.0	0.4	NA	4,340	100	Feed source

[a] NA, not applicable.
[b] Repeat analysis of the same sample.
[c] A process upset caused the endotoxin concentration of sample SDD-03-22 to be artificially low. Since the endotoxin concentration in feed, ~4,000 EU/ml, was confirmed using the same sample preparation procedure, this value was used to determine the percentage of endotoxin remaining.

showing the combinations of reactor tube length and flow rate selected for the temperature range used in this study.

Methodology development. Preliminary tests were conducted to evaluate system performance and establish a baseline. Particular attention was given to the tracing of an endotoxin standard to ensure uniform delivery into the system. All wetted surfaces of the final system were stainless steel components. In addition, the feed rate was optimized for the dual-piston pumps used in this test. The minimum endotoxin injection rate was maintained at 0.4 ml/min. The concentrated endotoxin had a concentration of ~550,000 EU/ml, which was based on the stock vial dilution. The water injection rate was adjusted accordingly to maintain a concentration of ~5,000 EU/ml.

The initial setup utilized a sterile needle (with a plastic base) to extract the reconstituted CSE from a sealed vial; as the CSE was removed, suction was created inside the vial, which could have altered the intended flow rate, thus affecting the overall concentration. To resolve this issue, the CSE was extracted from the open vial with a stainless steel tube. To monitor the feed rate of the concentrated endotoxin, the source vial was place on an analytical balance and its weight was monitored continuously throughout the test.

Scoping tests were conducted at room temperatures with a 0.6-m reactor to verify the overall concentration after incorporating changes into the test system. New data demonstrated acceptable performance of the test system. Another parameter evaluated during this test was the time dependence of feeding the endotoxin through the system. Based on residence time calculations, the residence time for the combined solution is relatively short (less than 10 s). The limiting factor was the time required for the concentrated endotoxin to get from the supply vial into the test loop (approximately 30 s). As observed in the data, the sample collected after 4 min was almost half the concentration of the sample collected after 8 min. After 8 min, there was no change in the concentration of

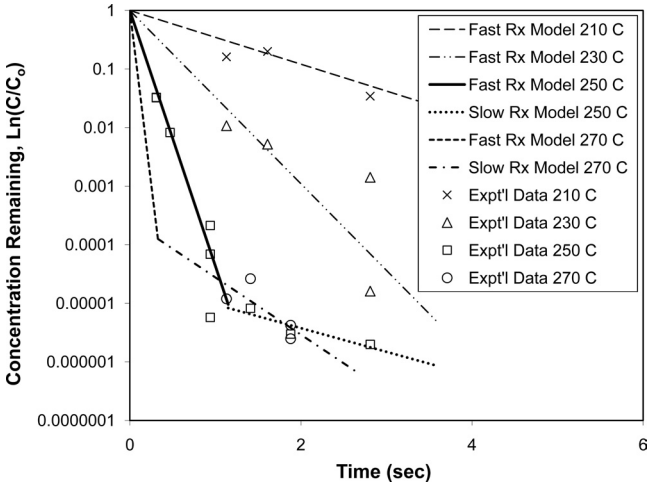

FIG. 3. Comparison of model predictions with experimental data for HTP depyrogenation. Rx, reaction.

the samples collected, indicating that a steady state was reached. Based on these results, future samples would be taken at least 8 min after initiating the endotoxin feed. Triethylamine (TEA) was mixed with the supply water for tests SDD-03-13 and SDD-03-14 to evaluate the effectiveness of a detergent. These results indicated no improvement to the normal feed water experiment, and therefore TEA was not used in subsequent tests.

RESULTS

Experimental data. The first set of seven samples was collected using the 1.2-m reactor. These data demonstrated that a minimum time may be required to reach a steady state after initiating the endotoxin feed before collecting a sample. As shown for samples SDD-03-17 and SDD-03-18 in Table 1, there is a difference of three times the concentration between these two samples where these samples were collected at 5 and 10 min, respectively. All of these samples were heated to 250°C, except for the last sample, which was used to determine the overall feed concentration. As shown in Fig. 3, the data follow a linear trend when plotted on a semilog scale, which is expected for depyrogenation data up to a 3- to 4-log reduction.

The second set of tests included eight samples collected at a combination of 270°C and 250°C using the 3.7-m reactor. The goal of this round of testing was to expand upon the data collected in the first round at 250°C to demonstrate a greater reduction of the endotoxin concentration. This test was successful in achieving a >5-log reduction of the endotoxin concentration.

The third set of tests included eight samples collected at a combination of 230°C and 210°C using the 3.7-m reactor. A 2- to 3-log reduction of the endotoxin concentration was achieved, which is reasonable for the operating temperatures and residence time.

Kinetic models. Most of the kinetic models reported in the literature deal with the inactivation of living organisms (2, 9, 11, 12, 39). Only a few papers have addressed kinetic models for the inactivation of endotoxins (5, 23, 24, 35). The commonality of inactivation of endotoxins and living organisms lies in that their kinetic trends are both not log linear in most cases. The pattern of microbial survival curves has been revisited and reinterpreted using Weibull distributions of resistance as a first approximation (30).

A freeware tool, GInaFiT (19), was used to assess non-log-linear microbial survival curves. Most of the data from this study were collected at 250°C, and as shown in Fig. 3, these data display a non-log-linear pattern similar to reported trends in microbial survival curves. To explore the applicability of this modeling tool and the suitability of the Weibull model, the data for the inactivation of endotoxins obtained from this study at 250°C were analyzed. Table 2 shows the model prediction results with an emphasis on comparing log-linear models with Weibull models. The classic Weibull model has greater prediction accuracy than the classic log-linear (Arrhenius) model. Introducing an additional parameter into both the Weibull and log-linear models produces a considerable improvement at the tail end. Double Weibull and biphasic, which require five and four parameters, respectively, have further improved prediction accuracy, but the improvement is much smaller. This small improvement comes at the expense of using more parameters. The figures of merit (mean sum of squared error [MSSE], root mean sum of squared error [RMSE], and R^2) show that the biphasic model is comparable to the Weibull + tail model in both prediction accuracy and the number of parameters used.

As shown in Fig. 3, 5-log endotoxin inactivation was achieved at 250°C in about 1 s of exposure, followed by a lower rate. A log-linear kinetic model would be convenient if the endotoxin inactivation range were limited to 3 to 5 logs. In addition, the two parameters for the Arrhenius log-linear kinetic model have meanings connected to chemical reactions, i.e., activation energy and frequency factor. The Arrhenius model is simple and can account for the temperature dependency of the reaction rate. Further attempts were made to correlate available data obtained at different temperatures. The data from this study were obtained at the upper temperature limit, while the data from three previous studies were considered to extend the lower temperature limits to 200°C (25), 190°C (1), and 120°C to 140°C (28). Figure 4 shows the Arrhenius plot, which follows a linear trend with $r^2 = 0.9875$. Using the slope ($-E_a/R$) and the intercept ln(A) obtained from Fig. 3, the activation energy (E_a) and the frequency factor (A) were calculated to be 118.3 kJ/mol and 6.547×10^{12} s^{-1}, respectively. It was found that the regression of the data from this study (210°C, 230°C, and 250°C) generated almost the same results ($E_a = 117.9$ kJ/mol and $A = 6.043 \times 10^{12}$ s^{-1}) as the model presented in Fig. 3, covering temperatures of 120°C to 250°C.

As shown in Fig. 3, the data points at 250°C with residence times of greater than 1 s and all of the data points at 270°C appear to fall into the slow-reaction zone. These data were further treated to generate reaction rate constants for 250°C and 270°C. Based on these reaction rate constants, E_a and A for the slow-reaction zone were calculated to be 104.2 kJ/mol and 2.373×10^{10} s^{-1}, respectively. These kinetic parameters are summarized in Table 3. The experimental and predicted data at 250°C show a convincing biphasic behavior (i.e., a fast-reaction phase followed by a slow-reaction phase) of the endotoxin inactivation process. Although no data at very short exposure times were collected at 270°C, the model predictions shown in Fig. 3 suggest that at 270°C, the transition from the

TABLE 2. Comparison of models of hydrothermal inactivation of *E. coli* at 250°C

Model	Log N_0	Log N_{RES}	Para3[a]	Para4	Para5	Para6	MSSE	RMSE	R^2	Reference
Log linear[b]	−1.15		$k_{max} = 4.78$				0.8348	0.9137	0.8266	7
Log linear + tail[c]	−0.18	−5.54	$k_{max} = 9.10$				0.0429	0.2070	0.9924	18
Biphasic[d]	−0.14		$k_{max1} = 9.40$	$k_{max2} = 0.90$	$f = 0.99997$		0.0354	0.1882	0.9947	10
Weibull[e]	0.23		$\delta = 0.07$	$P = 0.51$			0.3270	0.5718	0.9418	27
Weibull + tail[f]	0.02	−5.61	$\delta = 0.19$	$P = 0.84$			0.0322	0.1795	0.9952	2
Double Weibull[g]	0.02		$d_1 = 0.19$	$P = 0.86$	$d_2 = 4.81$	$\alpha = 5.08$	0.0266	0.1630	0.9961	14

[a] Para3 to Para6, parameters 3 to 6, respectively.
[b] $N/N_0 = e^{-k_{max} \cdot t}$.
[c] $N = (N_0 - N_{res}) \times e^{-k_{max} \cdot t} + N_{res}$.
[d] $N/N_0 = f \times e^{-k_{max1} \cdot t} + (1 - f) \times e^{-k_{max2} \cdot t}$.
[e] $N/N_0 = 10^{-(t/\delta)^p}$.
[f] $N = (N_0 - N_{res}) \times 10^{-(t/\delta)^p} + N_{res}$.
[g] $N = \frac{N_0}{(1 + 10^{\alpha})}[10^{-(t/\delta_1)^p + \alpha} + 10^{-(t/\delta_2)^p}]$.

fast to the slow reactions takes place sooner and at a shorter exposure time than that observed at 250°C.

***D* value.** The decimal reduction time is the time required at a given temperature to kill 90% of the organism population. By convention, the *D* value is used for sterilization processes, while log reduction (i.e., reduction by 1 logarithm unit) is used for depyrogenation processes. For convenience of discussion and simplicity of comparison, the terms *D* value and log reduction are used interchangeably in this context. The *D* value is calculated from the equation $D = 2.303\ k^{-1}$, where k is the reaction rate constant derived from the slope (slope $= -k$) of the survival curve on the semilog number of survivors versus exposure time chart. The *D* values, in seconds, calculated in this work are summarized in Table 3. For example, the *D* value at 250°C is 0.225 s. This means it would take about 1 s to achieve 5-log depyrogenation.

DISCUSSION

Kinetic data comparison. Our data comparison focused on the three most relevant works reported in the literature. The first one was the dry heat depyrogenation described by Tsuji and Harrison (35), whose work has often been cited as the benchmark for thermal depyrogenation processes. Tsuji and Harrison used the same endotoxin standard (*E. coli* O113:H10) and tested at temperatures of 170°C to 250°C. The *D* values reported by Tsuji and Harrison (35) are given in Table 3 as a comparison to those derived in this study. It should be noted that the *D* values for dry heat depyrogenation are in minutes and are about 2 orders of magnitude larger than those derived from the hydrothermal process presented in this work. Nevertheless, the ratios of *D* values of the slow- to the fast-reaction zones (i.e., D_2/D_1) from both wet heat and dry heat depyrogenation were plotted against temperature. As shown in Fig. 5, a linear trend is evident in the temperature range of 200°C to 270°C. Figure 6 further shows the first comparative semilog plot of the remaining concentration versus exposure time between the hydrothermal data and the dry heat data. The ratios of the inactivation rates for the fast to the slow zones are almost identical in both data sets.

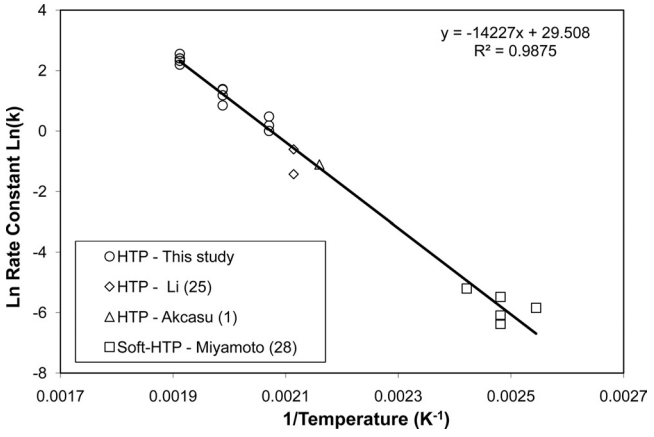

FIG. 4. Arrhenius plot of a first-order kinetic model of hydrothermal depyrogenation.

The second comparative semilog plot of the remaining concentration versus exposure time involves the data for moist heat at 121°C (5) and the data for soft HTP at 130°C with a steam saturation ratio of 1,000% (28), as shown in Fig. 6. The time in both data sets is in minutes, while the time for depyrogenation by HTP is in seconds. Figure 7 shows the experimental data (open symbols) and model predictions (lines). For the steam depyrogenation data, the slope of the line (the first-order reaction rate constant) for the slow-reaction zone (k_2) was calculated first. Since $D = 2.303\ k^{-1}$ and $D_2/D_1 = 0.058T - 3.75$ (Fig. 5), the reaction rate constant for the fast-reaction zone (k_1) was calculated from k_2 and D_2/D_1 at 121°C. As shown in Fig. 6, the model predictions appear to fit the data well. For the soft HTP data, there are only three data points which appear to be in the slow-reaction zone. Therefore, k_2 was calculated first and then k_1 was calculated by using the k_2 and D_2/D_1 values at 130°C. The solid symbols in Fig. 6 represent the model-predicted values in the fast-reaction zone. Overall, the biphasic reaction rate pattern appears to be characteristic of all three thermal systems for the inactivation of *E. coli*. The high depyrogenation rate at high temperatures typical of HTP appears to be a major advantage over the lower-temperature conventional depyrogenation processes.

Endotoxin inactivation mechanism. First, sterilization and endotoxin inactivation can be achieved by dry heat or moist

TABLE 3. Kinetic model parameters for thermal inactivation of *E. coli*

Process (source of data) and temp (°C)	Reaction zone	Frequency factor (1/s)	Activation energy (kJ/g mol)	D_1 (s)	D_2 (s)	D_2/D_1	Note
Wet heat depyrogenation (this work)							
200	Fast	6.55×10^{12}	118.3	4.07			Data from reference 25
210				2.18			Data
230				0.676			Data
250				0.229			Data
270				0.0842			Extrapolated
200	Slow	2.37×10^{10}	104.2		31.5	7.76	Extrapolated
210					18.2	8.35	Extrapolated
230					6.49	9.60	Extrapolated
250					2.47	10.9	Data
270					1.03	12.3	Data
Dry heat depyrogenation (reference 35)							
170	Fast		88.0	20.5			Data
190				12.4			Data
210				3.7			Data
230				0.99			Data
250				0.53			Data
170	Slow		82.2		170	8.29	Data
190					58.5	4.72	Data
210					29.4	7.95	Data
230					10.1	10.2	Data
250					5.6	10.6	Data

heat involving different mechanisms. While dry heat sterilization is thought to occur by the oxidation of essential cell constituents (13), moist heat kills microorganisms by coagulating and denaturing their enzymes and structural protein (42). The precise mechanistic steps of endotoxin inactivation are unknown but are likely to involve lipid A, which has been identified as the active site within LPS for pyrogenetic responses (26). For dry heat, the mechanism would be governed by gas-solid surface oxidative reactions and/or thermal decomposition reactions involving the active sites. Although both types of reactions may occur simultaneously, it is generally believed that oxidation is more dominant at lower temperatures while thermal decomposition becomes increasingly significant at higher temperatures. Conceptually, dry heat depyrogenation can be viewed as an extended process of dry heat sterilization to reach sterility, followed by rendering of the remaining cell fragments free of pyrogenicity.

Moist heat appears to have an intermediate impact on depyrogenation, as exhibited in the data of Bamba et al. (5). The rate of depyrogenation begins to accelerate with the

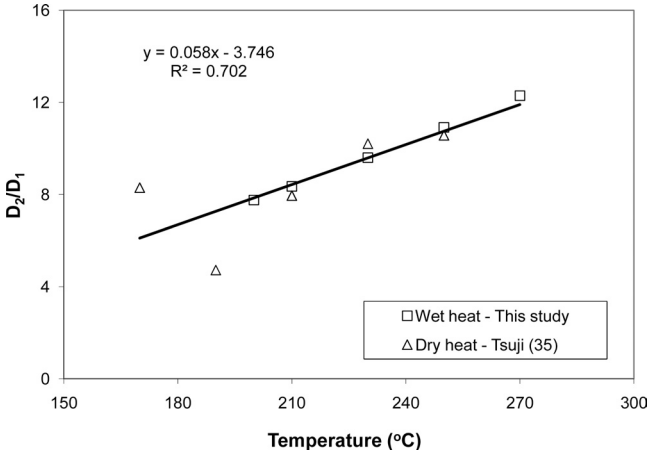

FIG. 5. Ratio of slow- and fast-reaction *D* values for wet and dry heat depyrogenation.

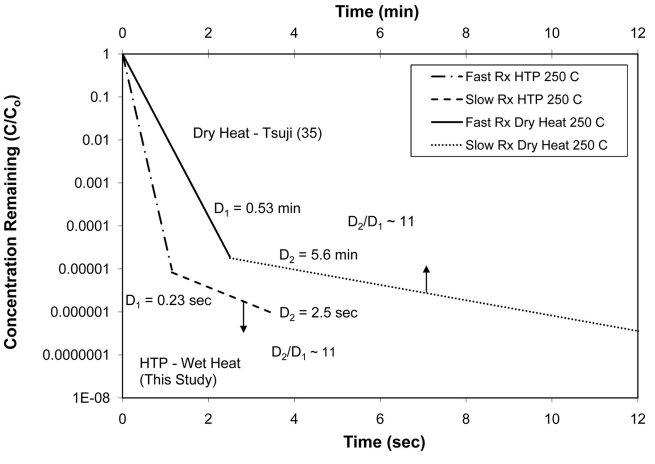

FIG. 6. Biphasic pattern of depyrogenation kinetics in wet and dry heat systems. Note that the vertical arrows indicate the corresponding *x* axes. Rx, reaction.

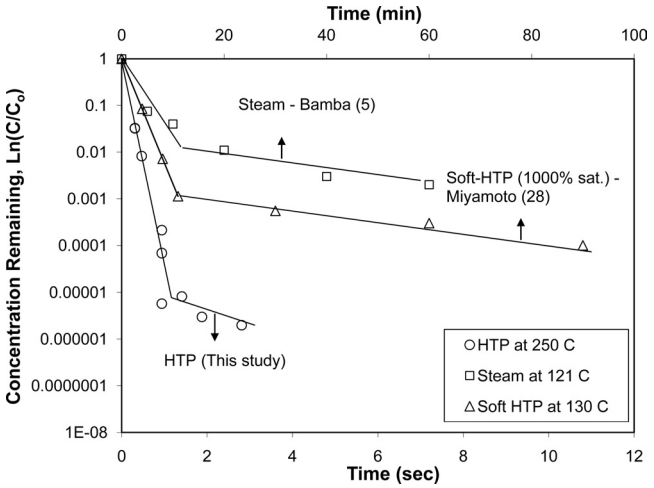

FIG. 7. Biphasic pattern of depyrogenation kinetics in wet heat systems. Note that the vertical arrows indicate the corresponding *x* axes. sat., saturation.

vapor phase, becoming more saturated, as demonstrated by Miyamoto et al., with the steam saturation ratio varying from 50% to 100% to 1,000% (28). As the temperature is further increased while the pressure is maintained above the saturation curve, the aqueous reaction medium begins to shift from being polar to being nonpolar (40). High-temperature water exhibits a lower dielectric constant and a lower ionization constant (pK_w) than liquid water under standard temperature and pressure conditions (8). For example, the static dielectric constant of saturated liquid water is 33.11, 30.01, 27.08, and 24.30 at 210°C, 230°C, 250°C, and 270°C, respectively (36), compared to a value of 80 for water at room temperature. The pK_w value is 11.2 at 250°C (6) compared to 14 at room temperature, suggesting a 3-log difference in the ion concentration product. This reversal solvent property makes high-temperature water a highly effective solvent for organic reactions that would not otherwise take place in room temperature water (17). For polymers, a good solvent is characterized by high degrees of the ability to penetrate and swell polymeric moieties. High-temperature water seems to function as an effective reactant and solvent for reactions involving lipid A. Therefore, HTP is a better process for endotoxin inactivation than dry heat and moist heat.

Unified representation. Figure 8 shows the temperature (*T*) and time (*t*) semilog correlation for 3 *D* heat sterilization and depyrogenation. The literature data were obtained from the independent studies described above (1, 5, 15, 21, 25, 28, 34, 35). All of the data shown in Fig. 8 are either actual experimental data or interpolated data corresponding to 3 *D* values. This chart can be used as a general design guideline that if the intercept of temperature (*T*) and time (*t*) falls in the region above and to the right side of a given line, a 3 *D* value will be achieved for the corresponding depyrogenation or sterilization process as indicated. For a given temperature, the wet heat depyrogenation is about 2 orders of magnitude more effective (i.e., less exposure time is required) than the dry heat depyrogenation process. Similarly, steam sterilization is about 1 order of magnitude more effective than the dry heat sterilization process. At the lower temperature limit, near 121°C, the data show that high steam saturation (28) shortens and low steam saturation (5, 28) prolongs the time required to achieve depyrogenation. Furthermore, the data confirm that depyrogenation requires a higher temperature or a longer time than sterilization. Therefore, the correlation developed for endotoxin inactivation can also serve as a conservative system design criterion for the sterilization process. The trends appear to be linear and show almost identical slopes on the *T-t* semilog chart, with the exception of autoclave sterilization, where only two typical data points at 121°C and 134°C are presented.

In summary, the major contributions of this study include (i) extending the temperature correlation of hydrothermal depyrogenation from the independent work of Bamba et al. (5) on

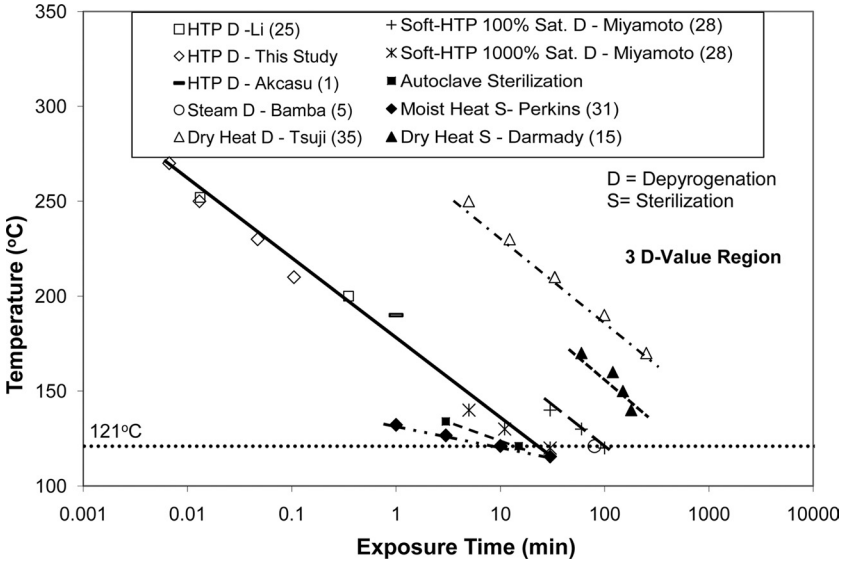

FIG. 8. Unified representation of depyrogenation and sterilization by wet and dry heat. Sat., saturation.

moist heat and Miyamoto et al. (28) on soft HTP at 120°C to 140°C to a higher a range of 210°C to 270°C, (ii) generating kinetic data to fill in the gap from an earlier HTP work by Li et al. (25) that explored depyrogenation by water at temperatures of up to 400°C, (iii) presenting a unified chart of new data and literature data related to depyrogenation and sterilization by hydrothermal (wet heat) and dry heat processes, and (iv) interpreting possible mechanisms involved in the HTP inactivation of endotoxins.

ACKNOWLEDGMENTS

This study was funded by U.S. Air Force contract FA8902-07-C-1012.

Annemie Geeraerd provided GInaFiT freeware (http://cit.kuleuven.be/biotec/). Brad Yundt assisted in setting up the Excel file for kinetic modeling.

REFERENCES

1. **Akcasu, A.** 1978. Preparation of pyrogen-free water. U.S. patent 4,070,289.
2. **Albert, I., and P. Mafart.** 2005. A modified Weibull model for bacterial inactivation. Int. J. Food Microbiol. **100:**197–211.
3. **Avallone, E. A., and T. Baumeister III.** 1996. Marks' standard handbook for mechanical engineers. McGraw-Hill, Boston, MA.
4. **Bamba, T., R. Matsui, and K. Watabe.** 1996. Effect of steam-heat treatment with/without divalent cations on the inactivation of lipopolysaccharides from several bacterial species. PDA J. Pharm. Sci. Technol. **50:**129–135.
5. **Bamba, T., R. Matsui, and K. Watabe.** 1996. Enhancing effect of non-ionic surfactant on the inactivation of lipopolysaccharide by steam-heat treatment. PDA J. Pharm. Sci. Technol. **50:**360–365.
6. **Bandura, A. V., and S. N. Lvov.** 2006. Static dielectric constant of water and steam. J. Phys. Chem. Ref. Data **35:**15–30.
7. **Bigelow, W. D., and J. R. Esty.** 1920. The thermal death point in relation to typical thermophilic organisms. J. Infect. Dis. **27:**602.
8. **Broll, D., et al.** 1999. Chemistry in supercritical water. Angew. Chem. Int. Ed. **38:**2998–3014.
9. **Buzrul, S., and H. Alpas.** 2004. Modeling the synergistic effect of high pressure and heat on inactivation kinetics of *Listeria innocua*: a preliminary study. FEMS Microbiol. Lett. **238:**29–36.
10. **Cerf, O.** 1977. Tailing of survival curves of bacterial spores. J. Appl. Bacteriol. **42:**1–19.
11. **Chen, H., and D. G. Hoover.** 2004. Use of Weibull model to describe and predict pressure inactivation of *Listeria monocytogenes* Scott A in whole milk. Innov. Food Sci. Emerg. Technol. **5:**269–276.
12. **Chen, G., O. H. Campanella, and C. M. Corvalan.** 2007. A numerical algorithm for calculating microbial survival curves during thermal processing. Food Res. Int. **40:**203–208.
13. **Chieppo, A., and T. Kupiec.** 2007. Sterilization: dry heat, p. 3512–3518. *In* J. Swarbrick (ed.), Encyclopedia of pharmaceutical technology, vol. 6, 3rd ed. Informa Healthcare USA, Inc., New York, NY.
14. **Coroller, L., I. Leguerinel, E. Mettler, N. Savy, and P. Mafart.** 2006. General model based on two mixed Weibull distributions of bacterial resistance for describing various shapes of inactivation curves. Appl. Environ. Microbiol. **72:**6493–6502.
15. **Darmady, E. M., K. E. A. Hughes, J. D. Jones, D. Prince, and W. Tuke.** 1961. Sterilization by dry heat. J. Clin. Pathol. **14:**38–44.
16. **Dawson, M. E.** 2005. Interference with LAL test and how to address it. LAL Update **22**(3)**:**1–5.
17. **Fraga-Dubreuil, J., and M. Poliakoff.** 2006. Organic reactions in high-temperature and supercritical water. Pure Appl. Chem. **78:**1971–1982.
18. **Geeraerd, A. H., C. H. Herremans, and J. F. Van Impe.** 2000. Structural model requirements to describe microbial inactivation during a mild heat treatment. Int. J. Food Microbiol. **59:**185–209.
19. **Geeraerd, A. H., V. P. Valdramidis, and J. F. Van Impe.** 2005. GInaFiT, a freeware tool to assess non-log-linear microbial survivor curves. Int. J. Food Microbiol. **102:**95–105.
20. **Gould, M. J., and T. J. Novitsky.** 1985. Depyrogenation by moist heat, p. 109–112. *In* PDA technical report 7: depyrogenation. Parenteral Drug Association, Inc., Bethesda, MD.
21. **Halls, N. A.** 1994. Achieving sterility in medical and pharmaceutical products. Marcel Dekker, New York, NY.
22. **Jacobs, P. H.** 1981. The use of reverse osmosis water for the production of parenterals in the hospital pharmacy. Pharm. World Sci. **3:**342–354.
23. **Lee, H., B. Zhou, W. Liang, H. Feng, and S. E. Martin.** 2009. Inactivation of *Escherichia coli* cells with sonication, manosonication, thermosonication, and manothermosonication: microbial responses and kinetics modeling. J. Food Eng. **93:**354–364.
24. **Lee, H., B. Zhou, H. Feng, and S. E. Martin.** 2009. Effect of pH on inactivation of *Escherichia coli* K12 by sonication, manosonication, thermosonication, and manothermosonication. J. Food Sci. **74:**E191–E198.
25. **Li, L., and J. J. Renard.** 2005. Process for producing sterile water for injection from potable water. U.S. patent 6,858,179.
26. **Lüderitz, D., et al.** 1975. Structure of lipopolysaccharides, the pyrogen of gram-negative bacteria, p. 10–20. International Symposium on Pyrogens. University College London, London, United Kingdom.
27. **Mafart, P., O. Couvert, S. Gaillard, and I. Leguerinel.** 2002. On calculating sterility in thermal preservation methods: application of the Weibull frequency distribution model. Int. J. Food Microbiol. **72:**107–113.
28. **Miyamoto, T., S. Okano, and N. Kasi.** 2009. Inactivation of *Escherichia coli* endotoxin by soft hydrothermal processing. Appl. Environ. Microbiol. **75:**5058–5063.
29. **Novitsky, T. J., and M. J. Gould.** 1985. Inactivation of endotoxin by polymyxin B, p. 93–97. *In* PDA technical report 7: depyrogenation. Parenteral Drug Association, Inc., Bethesda, MD.
30. **Peleg, M., and M. B. Cole.** 1998. Reinterpretation of microbial survival curves. Crit. Rev. Food Sci. **38:**353–380.
31. **Perkins, J. J.** 1969. Principles and methods of sterilization in health sciences, p. 71–73. Charles C Thomas, Springfield, IL.
32. **Seibert, F. B.** 2009. Pyrogens from an historical viewpoint. Transfusion **3:**245–249.
33. **Seibert, F. B.** 1923. Fever producing substance found in some distilled waters. Am. J. Physiol. **67:**90.
34. **Sweet, B. H., and J. F. Huxsoll.** 1985. Depyrogenation by dry heat, p. 101–108. *In* PDA technical report 7: depyrogenation. Parenteral Drug Association, Inc., Bethesda, MD.
35. **Tsuji, K., and S. Harrison.** 1978. Dry-heat destruction of liposaccharide: dry-heat destruction kinetics. Appl. Environ. Microbiol. **36:**710–714.
36. **Uematsu, M., and E. U. Franck.** 1980. Static dielectric constant of water and steam. J. Phys. Chem. Ref. Data **9:**1291–1306.
37. **U.S. Food and Drug Administration.** 1987. Guideline on validation of the Limulus amebocyte lysate test as an end-product endotoxin test for human and animal parenteral drugs, biological products, and medical devices. U.S. Food and Drug Administration, Silver Spring, MD.
38. **U.S. Pharmacopeial Convention.** 2008. The United States pharmacopeia 31. U.S. Pharmacopeial Convention, Inc., Rockville, MD.
39. **van Boekel, M. A. J. S.** 2002. On the use of the Weibull model to describe thermal inactivation of microbial vegetative cells. Int. J. Food Microbiol. **74:**139–159.
40. **Weingartner, H., and E. U. Franck.** 2005. Supercritical water as a solvent. Angew. Chem. Int. Ed. **44:**2672–2692.
41. **Welch, H., C. W. Price, V. L. Chandler, and A. C. Hunter.** 1943. The thermostability of pyrogens and their removal from penicillin. J. Am. Pharm. Assoc. **34:**114.
42. **Wood, R. T.** 2002. Fundamentals of thermal sterilization processes. Pharm. Biotechnol. **14:**191–212.